



# Ultrasound-based radiomics nomogram: A potential biomarker to predict axillary lymph node metastasis in early-stage invasive breast cancer



Fei-Hong Yu<sup>a</sup>, Jian-Xiang Wang<sup>a</sup>, Xin-Hua Ye<sup>a</sup>, Jing Deng<sup>a</sup>, Jing Hang<sup>a</sup>, Bin Yang<sup>b,\*</sup>

<sup>a</sup> Department of Ultrasound, The First Affiliated Hospital of Nanjing Medical University, Nanjing, China

<sup>b</sup> Department of Ultrasound, Jinling Clinical Medical College, Nanjing Medical University, Nanjing, China

## ARTICLE INFO

### Keywords:

Axillary lymph node metastasis  
Radiomics  
Ultrasonography  
Preoperative prediction

## ABSTRACT

**Purpose:** To establish a radiomics nomogram integrating clinical factors and radiomics features from ultrasound for the preoperative diagnosis axillary lymph node (ALN) status in patients with early-stage invasive breast cancer (EIBC). **Materials and methods:** Between September 2016 and December 2018, four hundred twenty-six ultrasound manually segmented images of patients with EIBC were enrolled in our retrospective study, which were divided into a primary cohort (n = 300) and a validation cohort (n = 126). A radiomics signature was built with the least absolute shrinkage and selection operator (LASSO) algorithm in the primary cohort. Multivariable logistic regression analysis was used to establish a radiomics nomogram model based on radiomics signature and clinical variables. The performance of nomogram was quantified with respect to discrimination and calibration. The radiomics model was further evaluated in the internal validation cohort.

**Results:** The radiomics signature, consisted of fourteen selected ALN-status-related features, achieved moderate prediction efficacy with an area under the curve (AUC) of 0.78 and 0.71 in the primary and validation cohorts respectively. The radiomics nomogram, comprising tumor size, US-reported LN status and radiomics signature, showed good calibration and favorite performance for ALN detection (AUC 0.84 and 0.81 in the primary and validation cohort). The decision curve which was demonstrated the radiomics nomogram displayed good clinical utility.

**Conclusion:** The radiomics nomogram could hold promise as a non-invasive and reliable tool in predicting ALN metastasis and may facilitate to develop more effective preoperative decision-making.

## 1. Introduction

Axillary lymph node (ALN) status is one of the most influential diagnostic and prognostic factor for disease free survival among early-stage invasive breast cancer (EIBC) with clinically negative axillary disease [1,3]. Clinicians once regarded that breast cancer's standard treatment was radical mastectomy plus axillary lymph node dissection (ALND), whereas as many as 70% of early breast cancer patients exhibit no ALN metastasis [2], and then in these cases, some types of axillary surgery can be considered as a significant overtreatment [3]. In recent years, sentinel lymph node biopsy (SLNB), which is less invasive than ALND, has replaced full ALND as a staging procedure in clinically lymph nodes negative patients [3,4] due to serious associated complications [5,6]. Sentinel lymph node is the first lymph node to receive

lymphatic drainage straightly from the primary tumor, thus SLNB offers a high accuracy of metastasis prediction to guide clinical decision making. Although SLNB has reduced significantly morbidity than ALND, the incidence rate of upper limb edema, weakened shoulder, arm pain, and numbness (3.5%, 3.5%, 8.1%, and 10.9%, respectively) is not negligible [6]. Furthermore, SLNB is associated with a potentially high false-negative rate, ranging from 5 to 10% [7]. Therefore, a noninvasive method is needed to evaluate ALN status and to safely avoid the use of SLNB in patients without ALN metastasis.

Axillary ultrasound (AUS) has long been a routine imaging modality for preoperatively evaluating axillary nodal status. US imaging shows acceptable accuracy for discriminate benign versus malignant breast tumors but is of limited value to help detect ALN metastasis, especially with minor axillary metastatic burden [8]. Previous studies [9,10] have

**Abbreviations:** ALN, axillary lymph node; ALND, axillary lymph node dissection; AUS, axillary ultrasound; AUC, area under the curve; DCA, decision curve analysis; CI, confidence interval; EIBC, early-stage invasive breast cancer; MRI, magnetic resonance imaging; LASSO, least absolute shrinkage and selection operator; ICC, interclass correlation coefficient; LN, lymph node; NAC, neoadjuvant chemotherapy; ROC, receiver operating characteristic curve; ROI, region of interest; SLNB, sentinel lymph node biopsy; VIF, variance inflation factor

\* Corresponding author at: Department of Ultrasound, Jinling Clinical Medical College, Nanjing Medical University, 305 Zhongshan East Road, 210002 Nanjing, Jiangsu, China.

E-mail address: [yangbin12yb@126.com](mailto:yangbin12yb@126.com) (B. Yang).

<https://doi.org/10.1016/j.ejrad.2019.108658>

Received 2 June 2019; Received in revised form 20 August 2019; Accepted 1 September 2019

0720-048X/© 2019 Elsevier B.V. All rights reserved.

used tumor and ALN characteristics to predict the presence of nodal metastases, such as tumor dimension, nonsmooth margins, cortical thickness and presence of fatty hilum loss, identified on US or magnetic resonance imaging (MRI). However, these imaging feature were visible to the naked eye according to macroscopic appearance on image grayscale, which limited its identification for more valuable microscopic image feature.

Radiomics is the process of conversion digital medical images into high-dimensional, mineable data. It involved high-throughput extraction of large numbers of quantitative imaging features to enhance accuracy of diagnosis, prognosis, and prediction, especially in oncology [11–13]. Previous studies [14,15] have suggested improvement in evaluating ALN in breast cancer using radiomics analysis of the primary tumor from dynamic contrast-enhanced MRI and mammography. To the best of our knowledge, there is no published report that has documented whether the value of radiomics signature from US would facilitate prediction of ALN metastasis in EIBC. Here, we investigated the potential use of US-based radiomics score as a predictive biomarker for the detection of ALN metastasis, and the purpose of the study was to develop and validate a US-based radiomics nomogram based on a combination of clinical factors and radiomics signature to predict the probability of ALN metastasis in early breast cancer patients.

## 2. Methods

### 2.1. Patients

This study was approved by our Institutional Review Board, and informed consent was waived for this retrospective research. Between September 2016 and December 2018, a total of 426 consecutive women who underwent breast surgery for EIBC were retrospectively reviewed according to the patient recruitment pathway. The US images and clinical data were collected from the data system of our hospital.

The inclusion criteria were as follows: (1) patients with clinical T1 or T2 primary invasive breast cancer confirmed after biopsy or resection, no palpable axillary adenopathy; (2) patients with a single solid tumor; (3) patients received SLNB/ALND; (4) the US examination obtained 2 weeks before surgery; (5) patients did not receive neoadjuvant chemotherapy (NAC) or biopsy prior to US examination. The exclusion criteria were as follows: (1) any intervention and preoperative therapy (radiotherapy, chemotherapy, ablation) before US examination; (2) patients with not completely visible region of interest (ROI) on the US images; (3) clinical data were incomplete. Fig. 1 displays recruitment pathway of the study population. Patients were grouped into primary and validation cohorts according to the order of the operation time. Enrolled 300 patients treated between September 1, 2016, and May 31, 2018 were included as the primary cohort, and 164 patients who underwent surgery between June 1, 2018 and December 31, 2018 were included as the validation cohort.

### 2.2. Clinical information

The following clinical characteristics, including age, lymph node (LN) status (the presence of macrometastasis or micrometastasis was defined as LN-positive), histologic tumor type, estrogen receptor status, progesterone receptor status and human epidermal growth factor receptor 2 status based on immunohistochemistry, were retrieved from medical records.

### 2.3. US image acquisition and US-reported LN status

US Images were acquired at our hospital using MyLab Twice (Esaote, Italy) ultrasound machine with a 5–13 MHz probe LA523. All the US examinations were performed by two experienced radiologists. For the target tumor, US-reported tumor size was defined by the largest diameter of the breast tumor measured on the grayscale US image, and tumor

shape (regular or irregular), margin (smooth or not) and US-reported LN status were evaluated and recorded. LN positive for suspicious metastasis was defined as irregular cortical thickness greater than 3 mm, longest/shortest axes ratio < 2 or absence of fatty hilum [16]. The two radiologists were blinded to the information on clinical and pathologic details, and any disagreement was resolved through consultation.

### 2.4. Region of interest segmentation, radiomics feature extraction and selection, signature construction

Region of interest (ROI) covering the whole tumor was manually delineated on the grayscale US image of the largest cross section using an open-source imaging platform (ITK-SNAP; <http://www.itksnap.org>). Three categories of features, including the basis of shape ( $n = 11$ ), first-order ( $n = 17$ ), and texture ( $n = 68$ ) features, were extracted automatically by using an in-house software (Pyradiomics version: <https://github.com/Radiomics/pyradiomics>) [17].

Interclass correlation coefficients (ICCs) were used to assess the intra- and interobserver reproducibility of radiomics feature extraction. To assess interobserver reliability, the ROI segmentation of 100 randomly chosen images in a blinded fashion was performed by two independent radiologists with 9 years (Reader 1) and 10 years (Reader 2) of experience in breast oncologic imaging. To evaluate intraobserver reliability, Reader 1 then repeated the same procedure one week later. The ICCs greater than 0.80 indicates good agreement of feature extraction. Least absolute shrinkage and selection operator (LASSO) logistic regression algorithm [18] was used to select LN status-related features with nonzero coefficients from among the 96 imaging features with penalty parameter tuning conducted by 10-fold cross-validation. Finally, a formula for the radiomics score was generated using a linear combination of the chosen features weighted by the LASSO method.

### 2.5. Construction and validation of the radiomics nomogram

On the basis of the multivariate logistic regression analysis, the clinical factors with  $P < 0.05$  were used to build the clinical model, and a radiomics nomogram incorporated the radiomics signature and the independent clinical risk factor was constructed and used as a quantitative tool to predict ALN status. The collinearity diagnosis of variables was performed using the variance inflation factor (VIF). When VIF is greater than 10, multicollinearity is considered to exist [19].

Receiver operating curves were plotted to evaluate the discrimination performance of established models, and the area under the curve (AUC) was calculated to quantify the discrimination of the nomogram. Calibration was plotted to explore the predictive accuracy of the nomogram by bootstrapping with 1000 resamples. The performance of internally validated of the radiomics nomogram was tested in the validation cohort, and a calibration curve was performed.

### 2.6. Development of decision-curve analyses

To evaluate the added clinical utility of radiomics nomogram in predicting ALN metastasis for EIBC patients, decision curve analysis (DCA) was performed by quantifying the net benefits for a range of threshold probabilities in the combined primary and validation dataset.

### 2.7. Statistical analysis

The Student's *t*-test or non-parametric Mann–Whitney *U* test was performed for continuous data. The Pearson chi-square or Fisher's exact test was used to compare the differences for the categorical variables. Statistical analysis was conducted with R software (version 3.3.4; <http://www.R-project.org>). A two-sided  $P < 0.05$  was considered significant. The statistical analysis packages are listed in the Supplementary material.

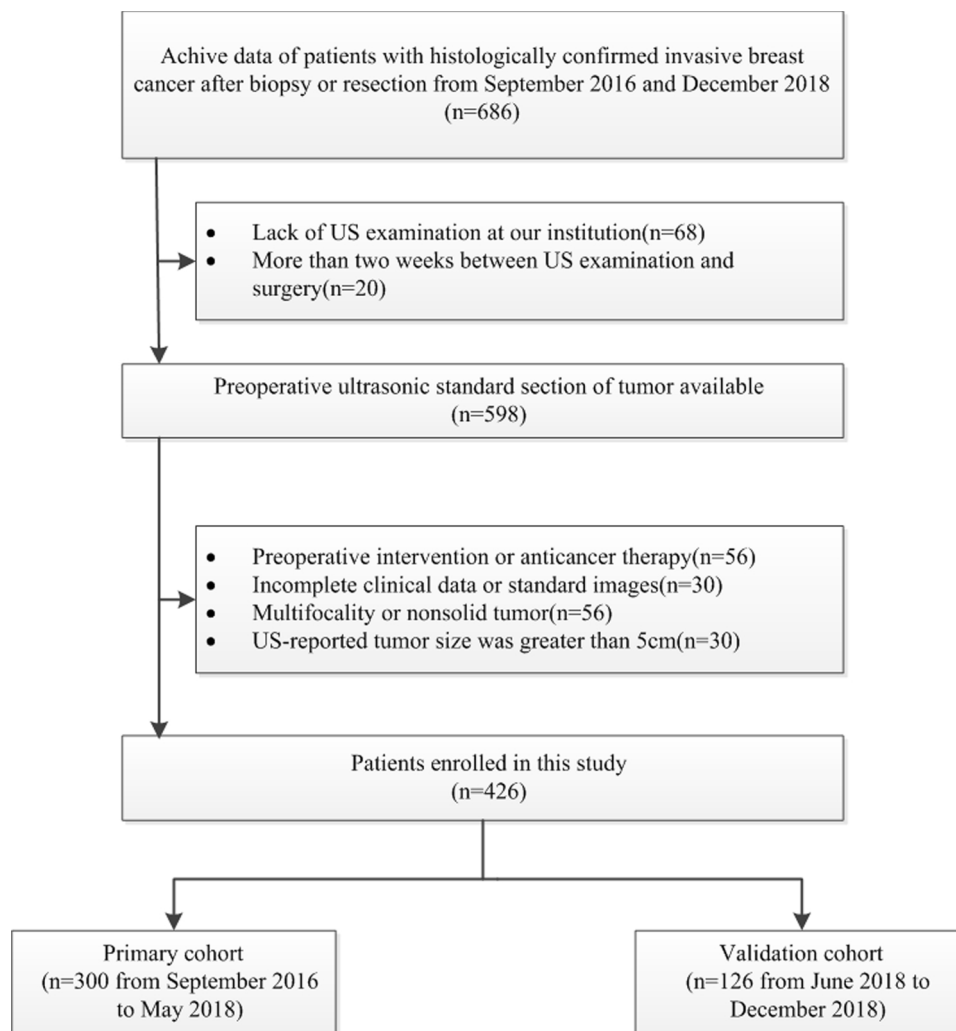


Fig. 1. Recruitment pathway for patients selection.

### 3. Results

#### 3.1. Clinic-pathological characteristics

Patient characteristics in primary and validation cohorts are summarized in Tables 1 and E1. There were no differences in clinic-pathological and ultrasonic characteristics between the two cohorts. LN metastasis patients formed 44.3% (133/300) and 41.3% (52/126) of the primary and validation cohorts, respectively. In total, 34.5% (67/194) of the patients without LN metastasis were overstaged and 25.0% (58/232) of the patients with LN metastasis were understaged according to US-reported status. The overall diagnostic accuracy of the US-reported LN status was 70.7% (301/426), for a sensitivity of 72.2% (174/241), specificity of 68.6% (127/185), positive predictive value of 75% (174/232), and negative predictive value of 65.5% (127/194).

#### 3.2. Radiomics signature building and diagnostic validation

A total of 96 imaging features were extracted from each grayscale US image. Using a LASSO logistic regression model, fourteen LN status-related features with nonzero coefficients were selected in the primary cohort (Fig. 2A and B). The radiomics score calculation formula is presented in the Supplementary material. The reproducibility of feature extraction was favorable, with intra-observer ICCs ranging from 0.81 to 0.91 and the inter-observe ICCs ranging from 0.79 to 0.90 respectively.

There was a significant difference in radiomics score between patients with and those without LN metastasis in the primary cohort (median, 0.49 vs  $-0.60$ ;  $P < 0.001$ ), which was then confirmed in the validation cohort (median, 0.25 vs  $-0.59$ ;  $P < 0.001$ ). The radiomics signature showed moderate predictive efficacy, with an AUC of 0.78 [95% confidence interval (CI), 0.73–0.83] in the primary cohort and 0.71 (95% CI, 0.62–0.80) in the validation cohort (Fig. 2C, D).

#### 3.3. Development and validation of prediction models

Table 2 shows the results of the multivariable regression analysis in the primary cohort. Regarding the collinearity diagnosis, the VIFs of the four predictors ranged from 1.15 to 1.45, indicating no multicollinearity. The clinical model was built with age, US-reported tumor size, US-reported LN status. The radiomics model with US-reported tumor size, US-reported LN status and radiomics signature was developed as a nomogram (Fig. 3).

Fig. 4A and B shows all receiver operating characteristic curves. The radiomics model showed the best discrimination in the primary cohort with the AUC reaching 0.84 (95% CI: 0.80–0.89), and the AUC value was higher than that of the clinical model and US-reported LN status alone (AUC, 0.76 [95%CI: 0.71–0.82],  $P < 0.001$ , AUC, 0.70 [95%CI: 0.64–0.76],  $P < 0.001$ , respectively). The radiomics model presented a similar AUC value (0.81 [95%CI: 0.74–0.88]) in the validation cohort, which suggested that the nomogram achieved better predictive efficacy than either the clinical model or the US-reported LN status alone (AUC,

**Table 1**  
Clinical characteristics of the primary and validation cohort.

Characteristic	Primary cohort (n = 300)			Validation cohort (n = 126)		
	Negative for LN metastasis (n = 167)	Positive for LN metastasis (n = 133)	P value	Negative for LN metastasis (n = 74)	Positive for LN metastasis (n = 52)	P value
Age			0.007			0.002
< 55	56(40.7)	75(56.4)		26(35.1)	33(63.5)	
> 55	111(59.3)	58(43.6)		48(64.9)	19(36.5)	
US-reported tumor size			< 0.001			0.046
T1 (< 2 cm)	73(43.7)	27(20.3)		33(44.6)	14(23.1)	
T2 (< 3 cm)	75(44.9)	44(33.1)		28(41.9)	20(36.5)	
T2(3–5 cm)	19(11.4)	62(46.6)		13(13.5)	18(40.4)	
Tumor shape			0.514			0.788
Regular	60(35.9)	43(32.3)		23(31.1)	15(28.8)	
Irregular	107(64.1)	90(67.7)		51(68.9)	37(71.2)	
Tumor margin			0.608			0.965
Smooth	38(22.8)	27(20.3)		14(18.9)	10(19.3)	
Non-smooth	129(77.2)	106(79.7)		60(81.1)	42(80.7)	
Histologic type			0.459			0.289
Ductal	106(63.4)	82(61.7)		51(68.9)	31(59.6)	
Lobular or mixed	56(33.5)	49(36.8)		20(27.0)	19(36.5)	
Other	5 (3.1)	2 (1.5)		3 (4.1)	2 (3.8)	
Estrogen receptor			0.853			0.747
Negative	30(18.0)	25(18.8)		14(18.9)	11(21.2)	
Positive	137(82.0)	108(81.2)		60(81.1)	41(78.8)	
Progesterone receptor			0.734			0.603
Negative	46(27.5)	39(29.3)		21(28.4)	17(32.7)	
Positive	121(72.5)	94(70.7)		53(71.6)	35(67.3)	
Her2			0.644			0.517
Negative	145(86.8)	113(84.9)		63(85.1)	42(80.8)	
Positive	22(13.2)	20(15.1)		11(14.9)	10(19.2)	
US-reported LN status			< 0.001			< 0.001
LN-negative	119(71.3)	41(30.8)		55(74.3)	17(32.7)	
LN-positive	48(28.7)	92(69.2)		19(25.7)	35(67.3)	
Radiomics score	−0.60(−1.69 to 0.49)	0.49(−0.47 to 1.45)	< 0.001	−0.59(−1.74 to 0.56)	0.25(−0.75 to 1.25)	< 0.001

Note: LN indicates Lymph node; US, Ultrasound; HER2, human epidermal growth factor receptor 2. Data are number of patients; data in parentheses are percentage. Data in the last line in parentheses are interquartile ranges.

0.75[95%CI: 0.66–0.83],  $P < 0.001$ , AUC, 0.71 [95%CI: 0.61–0.80],  $P < 0.001$ , respectively). The calibration curves demonstrated good consistency between predicted and observed LN metastasis in the primary and validation cohort (Fig. 3C, D). The Hosmer-Lemeshow test yielded a nonsignificant P value of 0.88 in the primary cohort and 0.93 in the validation set, suggesting no departure from the good fit. Therefore, our nomogram performed well in both the primary and validation cohorts.

On the basis of the maximum Youden index, the optimal cutoff value of all nomogram scores was defined to be 72(risk score is  $-0.129$ ), and all the patients were classified into low-risk and high-risk LN metastasis groups. Table E2 showed the discriminatory efficiency of ALN metastasis between the two groups ( $P < 0.001$ ). The sensitivity and specificity of the radiomics nomogram were 71.9% (133/185) and 81.3% (196/241) in the entire cohort, and positive predictive value and negative predictive value were 74.7% (133/178) and 79.0% (196/248) respectively. The DCAs based on the US-reported LN status, the clinical model and radiomics nomogram were shown in Fig. 5. The radiomics nomogram achieved the most clinical utility to predict ALN metastasis when the threshold probability for a patient is within a range from 0 to 0.79.

#### 4. Discussion

The aim of this study was to establish and validate a radiomics nomogram derived from clinical factors and imaging data, especially, radiomics features from US, for the preoperative diagnosis ALN status in patients with EIBC. The performance of the radiomics nomogram was good, which demonstrated the incremental value of the radiomics score, outperforming clinical model and macroscopic observations of ALN status using US (AUC of 0.84 vs 0.76 vs 0.70 in the primary cohort; 0.81 vs 0.75 vs 0.71 in the validation cohort).

Radiomics has shown promise in differentiate benign and malignant tumors [21], discriminating molecular subtypes [22], and predicting response to NAC [23] based on MRI or Computed tomography. However, recently increasing number of studies demonstrated ultrasound data can be used for radiomics analysis. For example, Wang et al. [24] assessed liver fibrosis in chronic hepatitis B and quantitatively analyzed the heterogeneity in two-dimensional shear wave elastography ultrasound images. Hu et al. [25] developed an US-based radiomics score to predict microvascular invasion in hepatocellular carcinoma. In our study, to avoid innate differences among the different type of US machines such as brightness or contrast, all of images in our study were from the same machine and performed by two experienced radiologists in order to standardize data extraction and acquisition. A radiomics signature, which expressed intratumor heterogeneity, was developed based on fourteen features extracted from US images. The new radiomics signature displayed adequate discriminative ability (AUC 0.78 in the primary cohort, 0.71 in the validation cohort), which was significantly associated with ALN metastasis ( $P < 0.001$ ). Among fourteen radiomics features, Kurtosis as a dominant features in our radiomics signature quantified intratumor heterogeneity. Yang et al. [26] demonstrated that Kurtosis had good performance in predicting LN malignancy among histogram parameters, which was likely to reduce false-positive cases when predicting LN status and could help to avoid unnecessary surgery. In addition, we identified four greylevel co-occurrence matrix (GLCM) parameters. GLCM features were known as the most commonly used texture parameters which are a combination of gray levels employing the number, distance, and angle. The present work [27] suggested that GLCM extracted from diffusion-weighted MRI showed strong correlations with LN metastasis, which was in line with our study. Meanwhile, radiomics features of biomedical image were associated with gene-expression profiles [28], which probed underlying

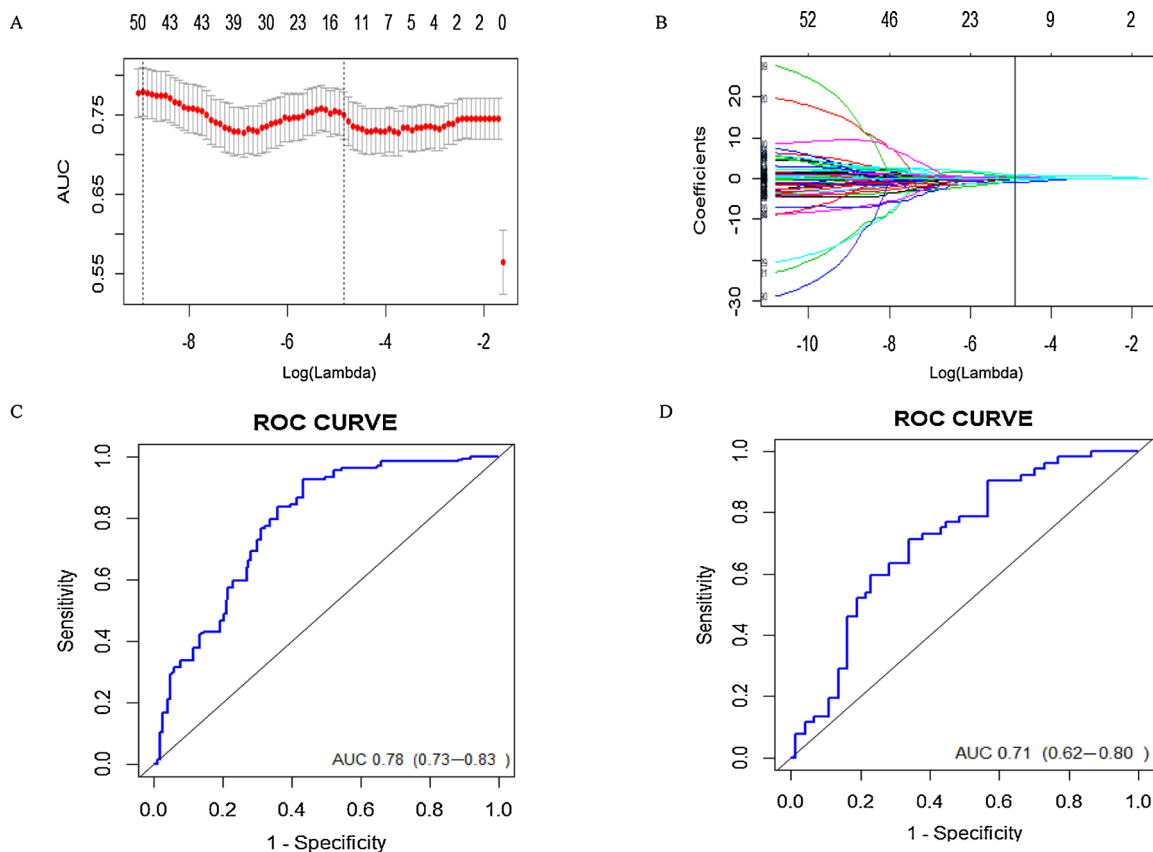


**Fig. 2.** Radiomics feature selection using LASSO logistic regression in the primary cohort and the predictive efficacy of the radiomics signature. **A.** Selection of the tuning parameter ( $\lambda$ ) in the LASSO model via 10-fold cross validation based on the 1 standard error of the minimum criteria (the 1-SE criteria). The value of  $\lambda$  that gave the minimum average binomial deviance was used to select features. Dotted vertical lines were drawn at the optimal values using the minimum criteria and the 1-SE criteria. The optimal  $\lambda$  value of 0.0075 with  $\log(\lambda)$  of  $-4.891$  was selected. **B.** LASSO coefficient profiles of the 96 radiomics features. Vertical line was drawn at the value selected using 10-fold cross-validation, where optimal  $\lambda$  resulted in 14 nonzero coefficients. Plots (C) and (D) show the ROC curves of the radiomics signature in the primary and validation cohort, respectively.

biologic mechanisms. Therefore, it is noteworthy that quantifiable features in the radiomics signature could assess intratumor heterogeneity and stratify patients on the basis of the statistical risk of LN metastasis.

We developed a nomogram that integrated radiomics signature with US-reported tumor size and US-reported LN status to further improve its predictive accuracy for ALN metastasis. Recently, several previous nodes have evaluated the likelihood of ALN status in patient with breast cancer with some clinicopathologic and genetic features, including lymphovascular invasion [2,29], the number of positive sentinel

lymph nodes [29] and miRNA [30], which may beyond clinical implication because we get such date only post-surgery or after immunohistochemical technique. Therefore, similar to Han’s et al. [15] research, the greatest advantage of our nomogram was that ALN status could be assessed non-invasively before surgery.

According to the proposed risk classifier, radiomics nomogram was able to categorize patients into low- and high-risk groups. As we know, ACOSOG Z0011 trial [31] suggested no benefit of completion axillary dissection for patients with no axillary lymph node involvement and one or two nodal metastases. Although ultrasound-guided lymph node

**Table 2**  
Risk factor for axillary lymph node metastasis in early-stage invasive breast cancer.

Variable	Clinical Model		Radiomics Model	
	Odds Ratio(95%CI)	P value	Odds Ratio(95%CI)	P value
age	1.73(1.02, 2.94)	0.042	0.70(0.37,1.33)	0.283
US-reported tumor size				
T1(< 2 cm)	Reference		Reference	
T2(< 3 cm)	0.58(0.32,1.07)	0.103	0.66(0.34,1.29)	0.232
T2(3–5 cm)	2.63(1.28, 5.45)	< 0.001	2.11(0.94,4.75)	0.006
US-reported LN status	3.13(1.76, 5.59)	< 0.001	4.26(2.20,8.27)	< 0.001
Radiomics score	NA	NA	5.35(3.13,9.18)	< 0.001

*Note:* US indicates Ultrasound; CI, Confidence interval. Data are results of the multivariable regression analysis. Data in parentheses are 95% confidence intervals. The clinical model was built based on independent predictors of axillary lymph node metastasis without radiomics signature.

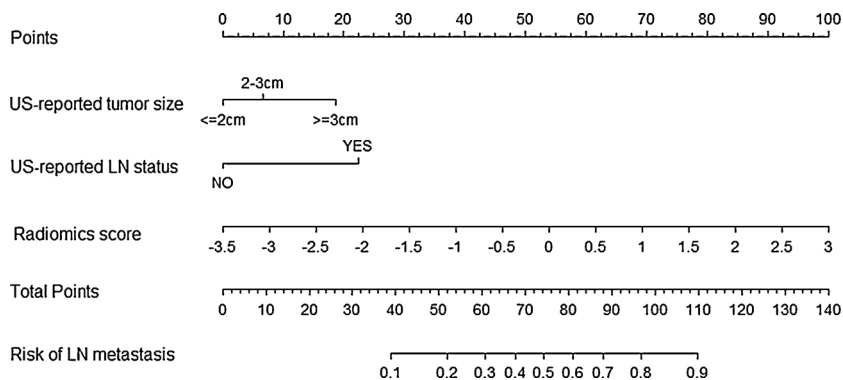


**Fig. 3.** A radiomics nomogram was developed with US-reported tumor size, US-reported LN status and radiomics signature for the prediction of ALN metastasis in the primary cohort.

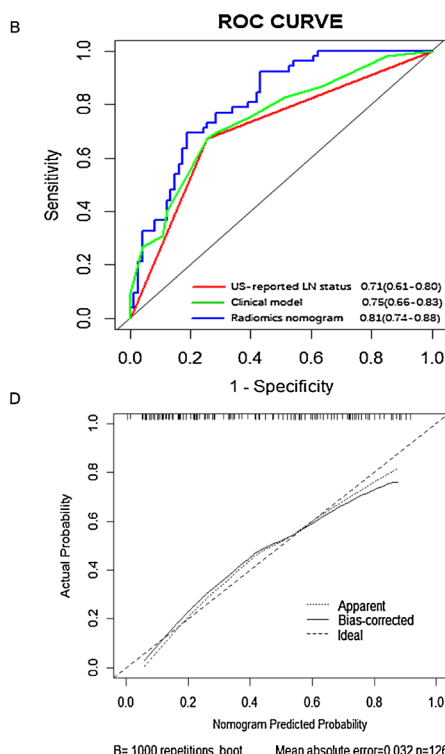
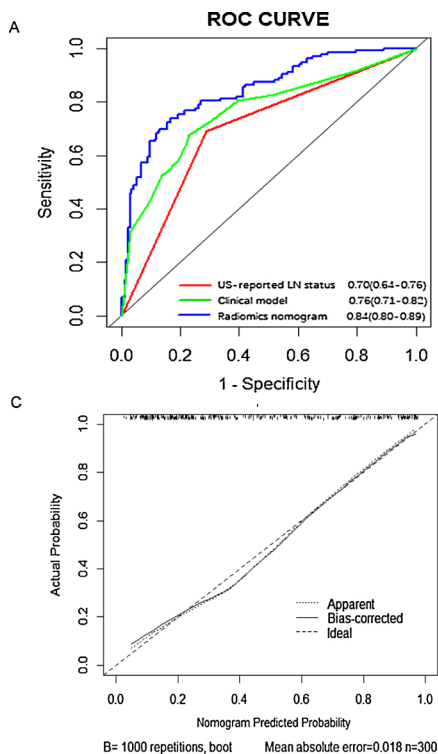


**Fig. 4.** A and B showed the comparison of receiver operating characteristic curves between the radiomics nomogram, clinical model and US-reported LN status in the primary and validation cohorts, respectively. Calibration curves of the radiomics nomogram in the primary cohort (C) and validation cohort (D). The 45 straight line represents a perfect match between the actual (Y-axis) and nomogram-predicted probabilities (X-axis), and the dotted lines represent the predictive performance of the nomogram. The closer distance between two curves, the better the predictive accuracy of the nomogram is.

biopsy was a standard process in preoperative assessment in patients with breast tumor, low sensibility in diagnosis SLN involvement affected its accurate evaluation due to the presence of inadequate samples. Oreste and Umberto [32] put forward a problem whether SLNB should be omitted in low-risk patients with clinical node-negative breast cancer, and the results of the trial reported that it was of great clinical relevance to select those patients that can safely avoid axillary surgery or should not undergo either a SLNB or an ALND, which further enhanced the significance of preoperative non-invasive model and offered a more tailored medical approach for improving patients' quality of life.

There are several limitations in our study. Firstly, our radiomics model established and validated for distinguishing ALN status was performed in a single hospital with the limited sample size, so future studies need to involve a larger sample size and carry out multicenter external validation. Secondly, as a retrospective research, although the our radiomics signature displayed adequate discriminative ability, radiomics

research using grayscale US image was still lack of reproducibility of radiomics score because we did not perform intensity standardization and directly used the default values. Also, we will further use three-dimensional ultrasound images for feature extraction, which may contain more radiomics features than the conventional two-dimensional images. Thirdly, our radiomics nomogram was developed according to features extracted from primary breast tumor instead of the LNs since most of these patients underwent surgery directly without a preoperative SLNB, and we were unable to match the pathologically metastatic LNs with suspicious LNs on the ultrasound image. Moreover, the research objects were the patients with a single lesion for better exploring the correlation between tumor heterogeneity and ALN metastasis.

In conclusion, a novel radiomics nomogram incorporated the identified clinical risk factors and radiomics signature has the potential to be used as a non-invasive approach for ALN metastasis prediction for EIBC, and it is expected to affect the treatment strategies and assist clinical decision making.

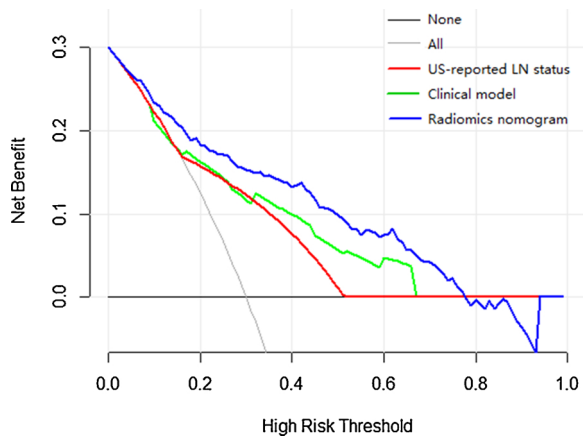


**Fig. 5.** Decision curve analysis for the each model in predicting ALN metastasis for EIBC patients. The y-axis measures the net benefit. The net benefit was calculated by subtracting the proportion of all patients who are false positive and summing proportion who are true positive, weighting by the relative harm of forgoing treatment compared with the harm of an unnecessary treatment [20]. The gray line represents the assumption that all patients have ALN metastasis (the treat-all scheme). The black line represents the assumption that no patients have ALN metastasis (the treat-none scheme). If the threshold probability is between 0 to 0.79, then using the radiomics nomogram (blue curve) to predict ALN metastasis adds more benefit for patients than all other models.

**Funding information**

No.

**Declaration of Competing Interest**

No.

**Acknowledgement**

No.

**References**

[1] D. Kolarik, V. Pecha, M. Skovajsova, et al., Predicting axillary sentinel node status in patients with primary breast cancer, *Neoplasma* 60 (2013) 334–342.  
 [2] J.L. Bevilacqua, M.W. Kattan, J.V. Fey, et al., Doctor, what are my chances of having a positive sentinel node? A validated nomogram for risk estimation, *J. Clin. Oncol.* 25 (2007) 3670–3679.  
 [3] G.H. Lyman, S. Temin, S.B. Edge, et al., Sentinel lymph node biopsy for patients with early-stage breast cancer: American Society of Clinical Oncology clinical practice guideline update, *J. Clin. Oncol.* 32 (2014) 1365–1383.  
 [4] G. Lyman, A. Giuliano, M. Somerfield, et al., American Society of Clinical Oncology guideline recommendations for sentinel lymph node biopsy in early-stage breast cancer, *J. Clin. Oncol.* 23 (2005) 7703–7720.  
 [5] J. Kootstra, J.E. Hoekstra-Weebers, H. Rietman, et al., Quality of life after sentinel lymph node biopsy or axillary lymph node dissection in stage I/II breast cancer patients: a prospective longitudinal study, *Ann. Surg. Oncol.* 15 (2008) 2533–2541.  
 [6] I. Langer, U. Guller, G. Berclaz, et al., Morbidity of sentinel lymph node biopsy (SLN) alone versus SLN and completion axillary lymph node dissection after breast cancer surgery, *Ann. Surg.* 245 (2007) 452–461.  
 [7] K. Kataria, A. Srivastava, D. Qaiser, What is a false negative sentinel node biopsy: definition, reasons and ways to minimize it? *Indian J. Surg.* 78 (2016) 369–401.  
 [8] S.C. Diepstraten, A.R. Sever, C.F. Buckens, et al., Value of preoperative ultrasound-guided axillary lymph node biopsy for preventing completion axillary lymph node

dissection in breast cancer: a systematic review and meta-analysis, *Ann. Surg. Oncol.* 21 (2014) 51–59.  
 [9] A.S. Caudle, H.M. Kuerer, H.T. Le-Petross, et al., Predicting the extent of nodal disease in early-stage breast cancer, *Ann. Surg. Oncol.* 21 (2014) 3440–3447.  
 [10] S.J. Hyun, E.K. Kim, H.J. Moon, et al., Preoperative axillary lymph node evaluation in breast cancer patients by breast magnetic resonance imaging (MRI): can breast MRI exclude advanced nodal disease? *Eur. Radiol.* 26 (2016) 3865–3873.  
 [11] P. Lambin, R.T.H. Leijenaar, T.M. Deist, et al., Radiomics: the bridge between medical imaging and personalized medicine, *Nat. Rev. Clin. Oncol.* 14 (2017) 749–762.  
 [12] S. Wu, J. Zheng, Y. Li, et al., A radiomics nomogram for the preoperative prediction of lymph node metastasis in bladder cancer, *Clin. Cancer Res.* 23 (2017) 6904–6911.  
 [13] R.J. Gillies, P.E. Kinahan, H. Hricak, Radiomics: images are more than pictures, they are data, *Radiology* 278 (2016) 563–577.  
 [14] J.B. Yang, T. Wang, L.F. Yang, et al., Preoperative prediction of axillary lymph node metastasis in breast cancer using mammography-based radiomics method, *Sci. Rep.* 9 (2019) 4429.  
 [15] L. Han, Y.B. Zhu, Z.Y. Liu, et al., Radiomic nomogram for prediction of axillary lymph node metastasis in breast cancer, *Eur. Radiol.* 29 (2019) 3820–3829.  
 [16] S.L. Koelliker, M.A. Chung, M.B. Mainiero, et al., Axillary lymph nodes: US-guided fine-needle aspiration for initial staging of breast cancer-correlation with primary tumor size, *Radiology* 246 (2018) 81–89.  
 [17] J.J.M. van Griethuysen, A. Fedorov, C. Parmar, et al., Computational radiomics system to decode the radiographic phenotype, *Cancer Res.* 77 (2017) e104–e107.  
 [18] W. Hansheng, L. Guodong, C. Tsai, Regression coefficient and autoregressive order shrinkage and selection via the lasso, *J. R. Stat. Soc.* 69 (2007) 63–78.  
 [19] R.M. O'Brien, A caution regarding rules of thumb for variance inflation factors, *Qual. Quant.* 41 (2007) 673–690.  
 [20] A.J. Vickers, A.M. Cronin, E.B. Elkin, et al., Extensions to decision curve analysis, a novel method for evaluating diagnostic tests, prediction models and molecular markers, *BMC Med. Inform. Decis. Mak.* 8 (2008) 53.  
 [21] S. Bickelhaupt, D. Paech, P. Kickingereder, et al., Prediction of malignancy by a radiomic signature from contrast agent-free diffusion MRI in suspicious breast lesions found on screening mammography, *J. Magn. Reson. Imaging* 46 (2017) 604–616.  
 [22] H. Li, Y. Zhu, E.S. Burnside, et al., Quantitative MRI radiomics in the prediction of molecular classifications of breast cancer subtypes in the TCGA/TCIA data set, *NPJ Breast Cancer* 2 (2016) pii: 16012.  
 [23] N.M. Braman, M. Etesami, P. Prasanna, et al., Intratumoral and peritumoral radiomics for the pretreatment prediction of pathological complete response to neoadjuvant chemotherapy based on breast DCE-MRI, *Breast Cancer Res.* 19 (2017) 57.  
 [24] K. Wang, X. Lu, H. Zhou, et al., Deep learning radiomics of shear wave elastography significantly improved diagnostic performance for assessing liver fibrosis in chronic hepatitis B: a prospective multicentre study, *Gut* 68 (2018) 729–741.  
 [25] H.T. Hu, Z. Wang, X.W. Huang, et al., Ultrasound-based radiomics score: a potential biomarker for the prediction of microvascular invasion in hepatocellular carcinoma, *Eur. Radiol.* 29 (2019) 2890–2901.  
 [26] L.Q. Yang, D. Liu, X. Fang, et al., Rectal cancer: can T2WI histogram of the primary tumor help predict existence of lymph node metastasis? *Eur. Radiol.* (2019), <https://doi.org/10.1007/s00330-019-06328-z>.  
 [27] Y.H. Dong, Q.J. Feng, W. Yang, et al., Preoperative prediction of sentinel lymph node metastasis in breast cancer based on radiomics of T2-weighted fat-suppression and diffusion-weighted MRI, *Eur. Radiol.* 28 (2019) 582–591.  
 [28] K.M. Panth, R.T. Leijenaar, S. Carvalho, et al., Is there a causal relationship between genetic changes and radiomics-based image features? An in vivo preclinical experiment with doxycycline inducible GADD34 tumor cells, *Radiother. Oncol.* 116 (2015) 462–466.  
 [29] T. Fujii, R. Yajima, H. Tatsuki, et al., Significance of lymphatic invasion combined with size of primary tumor for predicting sentinel lymph node metastasis in patients with breast cancer, *Anticancer Res.* 35 (2015) 3581–3584.  
 [30] S. Shiino, J. Matsuzaki, A. Shimomura, et al., Serum miRNA-based prediction of axillary lymph node metastasis in breast cancer, *Clin. Cancer Res.* 25 (2019) 1817–1827.  
 [31] A.E. Giuliano, K.K. Hunt, K.V. Ballman, et al., Axillary dissection vs no axillary dissection in women with invasive breast cancer and sentinel node metastasis: a randomized clinical trial, *JAMA* 305 (2011) 569–575.  
 [32] G. Oreste, V. Umberto, Abandoning sentinel lymph node biopsy in early breast cancer? A new trial in progress at the European Institute of Oncology of Milan (SOUND: Sentinel node vs Observation after axillary UltraSOUND), *Breast* 21 (2012) 678–681.